Rheol Acta (2013) 52:115–125
DOI 10.1007/s00397-012-0666-2

ORIGINAL CONTRIBUTION

Dielectric analysis of TiO_2-based electrorheological suspensions

Juan Wang · Kongshuang Zhao · Liping Zhang

Received: 10 June 2012 / Revised: 24 October 2012 / Accepted: 28 November 2012 / Published online: 6 January 2013

Abstract Dielectric behaviors of titanium dioxide (TiO_2)-based electrorheological (ER) suspensions with different particle concentrations and TiO_2 polymorphs were investigated in the frequency range of 40 Hz to 110 MHz. Two relaxations in kilohertz and megahertz frequency range were attributed to interface polarization between TiO_2 and silicone oil and ion pair polarization between dissociated counterions and fixed charges on TiO_2 surfaces, respectively. Dipolar coefficient D, which is related to the construction or structure of the colloid, changes after critical volume fraction $\phi_c \approx 0.05$, indicating that chain-like or network structures are formed by particles. Based on percolation model, the values of critical exponent suggest that particles may form two-dimensional percolation network. Furthermore, the effective dielectric mismatch parameter, β_{eff}, was calculated based on the obtained phase parameters. We found that rutile should have better ER activity than anatase. The main reason for weak ER activity of pure TiO_2 ER suspensions may due to poor conductivity properties of TiO_2 crystals.

Keywords TiO_2 electrorheological suspensions · Dielectric relaxation · Percolation · Effective dielectric mismatch parameters · Polarization theory

Introduction

Electrorheological (ER) fluid, which is made of polarizable particles in an insulating liquid, is a kind of special, smart suspension. Under a dc field, particles in ER fluid will be polarized to form a chain-like structure; therefore, the fluid will represent a tremendous increase in their viscosity and a phase transition from liquid-like state to solid-like state within milliseconds. The smart properties of ER fluid have contributed to making it an attractive topic in recent years (Winslow 1949; Hao 2001).

ER effect is due to the formation of chain-like structure by particles (Winslow 1949). Several hypotheses have been developed to explain the formation mechanism of chain-like structure, for example, electric double layer model (Klass and Martinek 1967), water/surfactant bridges mechanism (Stangroom 1983), dielectric loss model (Hao et al. 2001), and polarization model (Parthasarathy and Klingenberg 1996). Each of these models, however, has its limitations, and the polarization model has been used widely in many researches because it is one of the most acceptable models to describe the mechanism. According to the polarization model, ER effect is contorted by dielectric mismatch defined by the relationship (Parthasarathy and Klingenberg 1996) $\beta = (\varepsilon_p - \varepsilon_a)/(\varepsilon_p + \varepsilon_a)$ (where ε_p and ε_a are the permittivity of particles and continuous medium in the fluid, respectively). The higher the dielectric mismatch, the stronger the ER effect is. Therefore, the dielectric properties of suspensions should dominate the ER effect. Many research studies have concentrated on how the particles' dielectric properties influence the ER effect. It is well known that Maxwell–Wagner polarization plays an important role to induce forces between particles and is the essential reason of the ER effect (Hao et al. 2001; Parthasarathy and Klingenberg 1996). Ikazaki et al. (1998) reported that the characteristic frequency of a good ER fluid should be between 100 and 10^5 Hz. Hao (2002) developed a theoretical approach to prove that a large dielectric loss is experimentally necessary for the ER response. All the

J. Wang · K. Zhao (✉) · L. Zhang
College of Chemistry, Beijing Normal University,
Beijing 100875, China
e-mail: zhaoks@bnu.edu.cn

works above showed the inherent and natural connection between the dielectric properties of suspension and its ER effect. Actually, although the ER effect of a fluid is studied mainly using the rheological measurements, its estimate is usually proved by dielectric spectroscopy method (Cheng et al. 2008, 2009; Liu et al. 2010; Yin and Zhao 2006; Wang et al. 2007). Besides, some valuable information such as dielectric parameters and phase parameters can also be obtained by analyzing dielectric spectroscopy (Zhao et al. 2002). These parameters especially the phase parameters of the suspension directly decide the values of dielectric increment (Hanai et al. 1977) and dielectric mismatch parameters (Parthasarathy and Klingenberg 1996), which are important to ER effect.

Titanium dioxide (TiO_2) is widely investigated as dispersion materials in ER fluid due to its high permittivity. Rheological studies have found that the ER activity of pure TiO_2 suspension is weak (Yin and Zhao 2006; Wang et al. 2007). Hence, many modified ways, such as doping metals or ions (Yin and Zhao 2004, 2006), doping conducting polymers (Cheng et al. 2009), and enhancing the interface or surface properties of particles (Liu et al. 2010; Wang et al. 2007), have been employed to improve the ER activity of TiO_2. As discussed above, the reason of weak ER effect for pure TiO_2-based ER suspensions must be related to the dielectric properties of TiO_2 (Yin and Zhao 2002). Therefore, in order to provide some positive information to its electrorheological properties, it is necessary to study TiO_2-based ER suspensions by dielectric analysis. However, to the authors' knowledge, the works on dielectric analysis of TiO_2 suspensions are rare.

In this work, dielectric behaviors of TiO_2-based ER suspensions with different concentration of particles and different TiO_2 polymorphs were investigated in the frequency range of 40 Hz to 110 MHz. We discussed the relaxation mechanism and structure changes of TiO_2 suspensions and tried to find out how particle concentrations and TiO_2 polymorphs influenced the dielectric properties and structures of ER suspensions. Moreover, according to the modified polarization model, effect dielectric mismatch parameter, β_{eff}, was calculated and the reason of weak ER activity for pure TiO_2-based ER suspensions was also discussed.

Materials and methods

Materials and preparation of ER suspensions

Three samples of commercial TiO_2 particles available from Aladdin Chemistry Co. Ltd. were used for preparation of the suspensions. Some properties of used particles are listed in Table 1.

Table 1 Physical properties of TiO_2 particles

Type of TiO_2	Average grain diameter (nm)	Surface treatment
Rutile, hydrophilic	100	Silica
Anatase, hydrophilic	100	Silica
Mixed (rutile + anatase)	100	Silica

Rutile and anatase are two different polymorphs of TiO_2. They all belong to tetragonal system but with different lattice parameters: $a = 4.575$ Å and $c = 2.987$ Å for rutile and $a = 3.771$ Å and $c = 9.688$ Å for anatase (Labat et al. 2007). All particles were further dehydrated in a vacuum at 120 °C for 12 h. The methyl silicone oil (viscosity $\eta = 350 \pm 8$ mPa s, density $\rho = 0.965$–0.975 g cm^{-3} at 25 °C) was dried before being used. Suspensions at series concentrations (1–40 wt%) for these three types of TiO_2 were prepared by incorporating the powders into the silicone oil by stirring with a Heidolph Diax-900 stirrer and then sonicating in an ultrasound bath for 2 min prior to dielectric measurement. In "Results and discussion" section, because the qualitative or quantitative equations we used are all related to particle volume fraction, we also calculated the volume fraction, and the volume fractions of TiO_2 in these suspensions were 0.25–19 vol%.

Dielectric measurement

Dielectric measurements were carried out with an HP 4294A Precision Impedance Analyzer (Agilent Technologies) which covers a frequency range of 40 Hz to 110 MHz and was controlled by a personal computer. The amplitude of the applied alternating field was 500 mV. The measurement temperature was 20 ± 0.1 °C. A dielectric cell with parallel stainless steel electrodes was employed to load the samples. The distance between the electrodes is 0.45 mm. All the experimental data were corrected for errors arising from stray capacitance (C_r), the cell constant (C_l), and residual inductance L_r. They are 0.64 pF, 0.24 pF, and 1.84E-7 (in farads per square siemens), respectively, determined with water, ethanol, and air.

The measured experimental data, capacitance C_x and conductance G_x, were corrected by using the following equations (Schwan 1963):

$$C_s = \frac{C_x\left(1+\omega^2 L_r C_x\right) + L_r G_x^2}{\left(1+\omega^2 L_r C_x\right)^2 + (\omega L_r G_x)^2} - C_r \tag{1}$$

$$G_s = \frac{G_x}{\left(1+\omega^2 L_r C_x\right)^2 + (\omega L_r G_x)^2} \tag{2}$$

where ω ($\omega = 2\pi f$, where f is the measurement frequency) is the angular frequency and the subscripts x and s denote

the directly measured and modified values, respectively. The obtained data of capacitance C_s and conductance G_s at each frequency were converted to permittivity and conductivity, using the following equations: $\varepsilon = C_s/C_l$ and $\kappa = G_s\varepsilon_0/C_l$ (ε_0 $(= 8.8541 \times 10^{-12}$ F/m) is the vacuum permittivity).

The dielectric response of a system in an applied electric field can be characterized by the complex permittivity ε^* which is defined as (Van Beek 1967)

$$\varepsilon^*(\omega) = \varepsilon(\omega) - j\frac{\kappa(\omega)}{\varepsilon_0\omega} = \varepsilon(\omega) - j\varepsilon''(\omega) - j\frac{\kappa_l}{\varepsilon_0\omega} \quad (3)$$

where $\varepsilon(\omega)$ and $\kappa(\omega)$ are the frequency-dependent real part of complex permittivity and complex conductivity, respectively, of the TiO_2 suspensions mentioned above, and $j = (-1)^{1/2}$. κ_1 is the low-frequency limit of conductivity (dc conductivity) and can be read directly from low-frequency plateau in $\kappa \sim f$ plot. $\varepsilon''(\omega)$ is the dielectric loss:

$$\varepsilon'' = \frac{\kappa(\omega) - \kappa_1}{\varepsilon_0\omega}. \quad (4)$$

Contribution of dc conductivity always causes electrode polarization in dielectric spectra. However, for some system, such as particles disperse in non-conductivity continuous phase, electrode polarization in dielectric spectra is not distinct and the dc conductivity κ_1 is negligible. In this case, Eq. 4 can be simplified as

$$\varepsilon'' = \frac{\kappa(\omega)}{\varepsilon_0\omega}. \quad (5)$$

Determination of dielectric parameters from dielectric spectra

In the present work, the Cole–Cole equation including two Cole–Cole terms was employed (Cole and Cole 1941):

$$\varepsilon^* = \varepsilon_h + \frac{\Delta\varepsilon_l}{1 + (j\omega\tau_l)^{\alpha_l}} + \frac{\Delta\varepsilon_h}{1 + (j\omega\tau_h)^{\alpha_h}} \quad (6)$$

where ε_h is the high-frequency limits of permittivity. The subscripts l and h denote the low- and high-frequency relaxation modes, respectively. $\Delta\varepsilon$, τ ($\tau = 1/2\pi f_0$, where f_0 is the characteristic relaxation frequency), and $\alpha(0 < \alpha \leq 1)$ are the dielectric increment, relaxation time, and Cole–Cole parameter indicating the distribution of relaxation time of each relaxation mode, respectively. $\Delta\varepsilon_l = \varepsilon_l - \varepsilon_m$ and $\Delta\varepsilon_h = \varepsilon_m - \varepsilon_h$, where ε_l and ε_m are low- and middle-frequency limits of permittivity, individually.

The dielectric parameters $\Delta\varepsilon$, τ, and α characterizing the dielectric behaviors of the suspensions can be obtained by fitting the Cole–Cole empirical Eq. 6 to the experimental data. The uncertainties of fitting process are of the order of ±1 to 2 %.

Moreover, the middle-frequency limits of conductivity, κ_m, was calculated using the following equation derived based on the reference Hanai et al. (1977):

$$\kappa_m = (\varepsilon_l - \varepsilon_m)\, 2\pi f_{0l}\varepsilon_0 + \kappa_l. \quad (7)$$

Dielectric model and determination of phase parameters

Figure 1 describes the dielectric model of spherical particles (radius R, complex permittivity ε_p^*, and complex conductivity κ_p^*) dispersed in a continuous medium $(\varepsilon_a^*\kappa_a^*)$ to form a whole suspension system with ε^* and κ^*. ϕ is the volume fraction of particles. ε_p^*, κ_p^*, ε_a^*, and κ_a^* are the parameters of constituent phase, i.e., so-called phase parameters.

The interfacial polarization of spherical particle suspensions can be well described by the Hanai's equation (Hanai et al. 1977):

$$\left(\frac{\varepsilon^* - \varepsilon_p^*}{\varepsilon_a^* - \varepsilon_p^*}\right)\left(\frac{\varepsilon_a^*}{\varepsilon^*}\right)^{1/3} = 1 - \phi. \quad (8)$$

After separating the real and image parts of Eq. 8, the phase parameters ε_p, ε_a, κ_p, and κ_a are related to the dielectric parameters ε_l, ε_m, κ_l, and κ_m as

$$\left(\frac{\varepsilon_m - \varepsilon_p}{\varepsilon_a - \varepsilon_p}\right)\left(\frac{\varepsilon_a}{\varepsilon_m}\right)^{1/3} = 1 - \phi \quad (9)$$

$$\varepsilon_l\left(\frac{3}{\kappa_l - \kappa_p} - \frac{1}{\kappa_l}\right) = 3\left(\frac{\varepsilon_a - \varepsilon_p}{\kappa_a - \kappa_p} + \frac{\varepsilon_p}{\kappa_l - \kappa_p}\right) - \frac{\varepsilon_a}{\kappa_a} \quad (10)$$

$$\kappa_m\left(\frac{3}{\varepsilon_m - \varepsilon_p} - \frac{1}{\varepsilon_m}\right) = 3\left(\frac{\kappa_a - \kappa_l}{\varepsilon_a - \varepsilon_p} + \frac{\kappa_l}{\varepsilon_m - \varepsilon_p}\right) - \frac{\kappa_a}{\varepsilon_a} \quad (11)$$

$$\left(\frac{\kappa_l - \kappa_p}{\kappa_a - \kappa_p}\right)\left(\frac{\kappa_a}{\kappa_l}\right)^{1/3} = 1 - \phi. \quad (12)$$

Details and procedural calculations for the Eqs. 8–12 are described elsewhere (Zhao et al. 2002; Hanai et al. 1977), by which the phase parameters for all the systems were obtained.

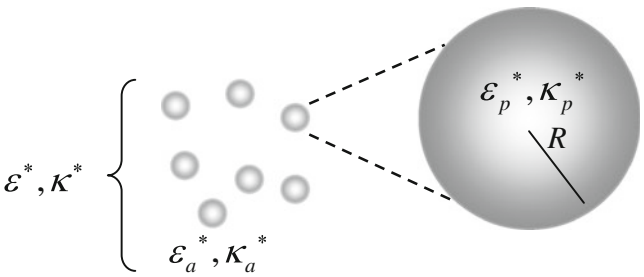

Fig. 1 Dielectric model of the suspensions

Results and discussion

Dielectric spectra and relaxation mechanism of TiO_2-based ER suspensions

Dielectric spectra of TiO_2-based ER suspensions with different particle concentrations

Figure 2 is the three-dimensional representations of the dependence of particle concentrations ranging from 1 to 40 wt% on dielectric loss spectra for rutile TiO_2-based ER suspensions. From Fig. 2, it is clear that a dielectric relaxation with a distribution at about 10^3–10^4 Hz can be observed and the relaxation shifts to a higher frequency range slightly with the increase of particle concentrations. The relaxation strength is also increased with particle concentrations. In order to confirm the mechanism of relaxations that occur in distributed dielectric spectra, we have tried different functions. We found that a deviation exists in high-frequency range no matter what type of function, single C-C function or single HN function (Havriliak and Negami 1967; Schönhals et al. 2009), is adopted to fit the spectra, indicating that some sub-relaxations exist in high frequency. Therefore, the two Cole–Cole functions (Eq. 6) were used to fit the dielectric data. Figure 3 is a sample of the best fitting of real part and imaginary part of permittivity for rutile TiO_2 suspension at 25 wt%. From Fig. 3b, it is obvious that within the investigated frequency range, the main relaxation consists of two sub-relaxations

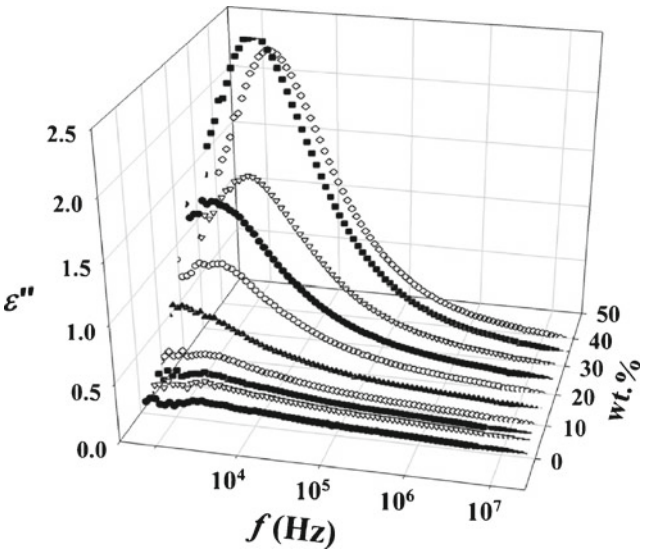

Fig. 2 Three-dimensional representations of the dependence of particle concentrations ranging from 1 to 40 wt% on dielectric loss spectra for rutile TiO_2 suspensions at 20 °C. The axis of frequency is logarithmic

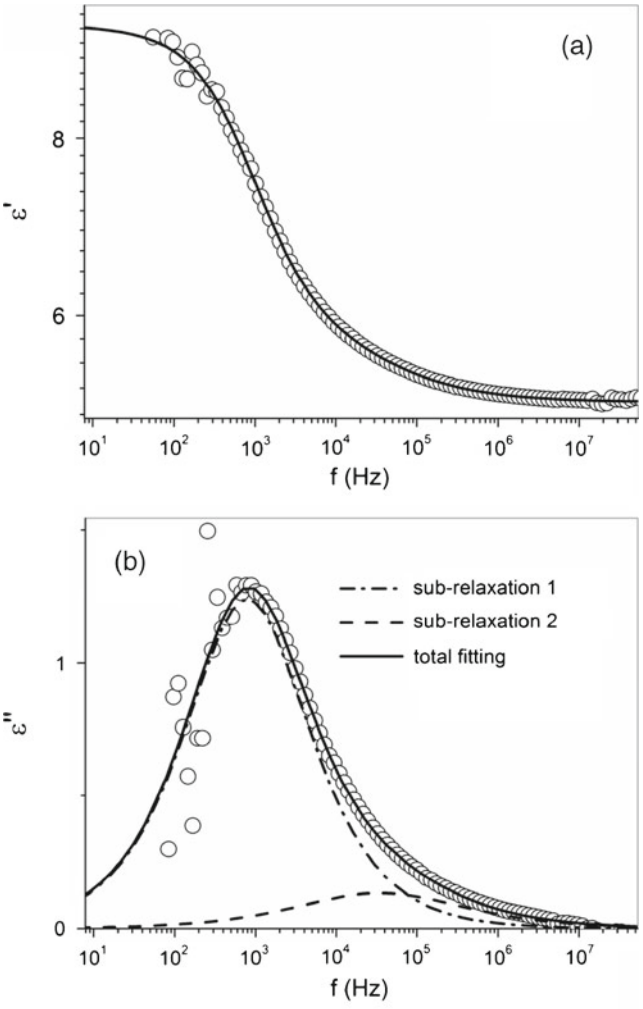

Fig. 3 Real part (**a**) and imaginary part (**b**) of rutile TiO_2 suspension at 25 wt%. The experimental data are indicated by *open circles* and the *solid line* is the best fit to Eq. 6

called sub-relaxation 1 and sub-relaxation 2 from low- to high-frequency, respectively, and the dielectric increment of the sub-relaxation 1 is significantly more than that of sub-relaxation 2.

Dielectric spectra of TiO_2-based ER suspensions with different TiO_2 polymorphs

Figure 4 shows the frequency dependences of permittivity (a) and dielectric loss (b) for rutile (open squares), anatase (open circles), and mixed (open triangles) TiO_2 suspensions. From Fig. 4, it can be seen that the relaxation behaviors for three polymorphs of TiO_2 suspensions are different. The dielectric increment $\Delta\varepsilon$, relaxation frequency f_0, dielectric loss ε'' of the three suspensions all follow the order of rutile > mixed > anatase.

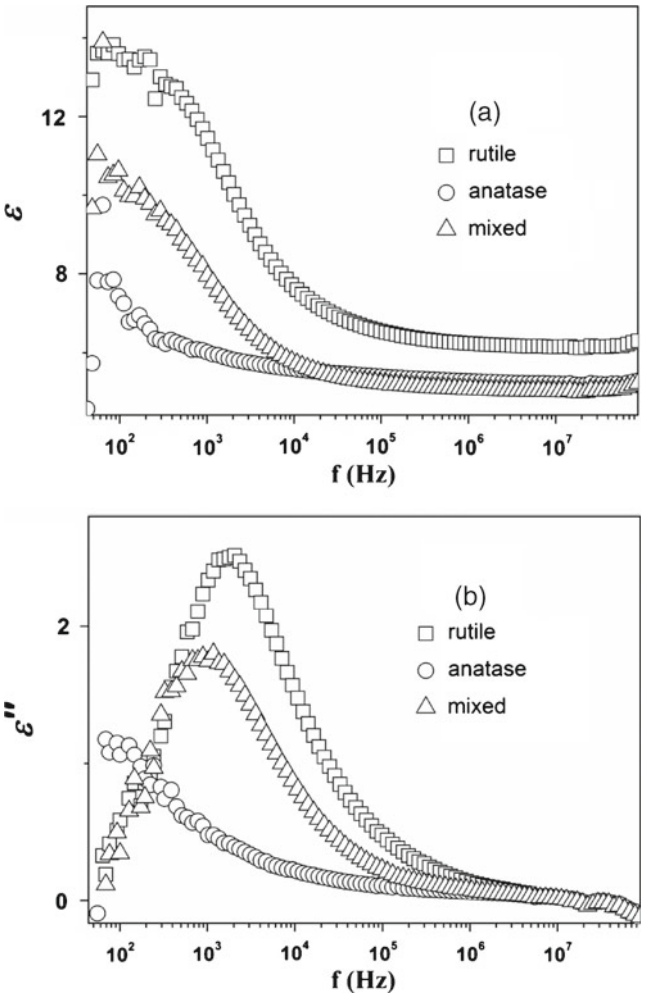

Fig. 4 Frequency dependences of permittivity (**a**) and dielectric loss (**b**) for rutile (*open squares*), anatase (*open circles*), and mixed (*open triangles*) TiO_2 suspensions. The particle concentration is 35 wt%

The mechanisms of high- and low-frequency dielectric relaxations

It is well known that the Maxwell–Wagner interface polarization plays an important role to induce forces between particles and it is the essential reason of ER effect (Hao et al. 2001; Parthasarathy and Klingenberg 1996). Therefore, to discuss the ER effect of fluid, it is necessary to clarify the mechanisms of relaxations observed in our study. As a typical collide suspension, the observed relaxation may be attributed to many relaxation mechanisms. The most likely mechanisms that will be considered are the Maxwell–Wagner (MW) polarization (Hanai et al. 1977) and counterion polarization (i.e., polarization of electric double layer) (Dukhin and Shilov 1974). For the suspensions of the particle disperse in water, the relaxation caused by polarization of an electric double layer usually appears around kilohertz, whereas MW polarization usually occurs at about 10^4–10^8 Hz. However, in our studied systems, no salts are added in the suspensions and the continuous phase is oil. Comparing with polarity of water, the significant decrease of polarity of silicon oil leads to a decrease of dissociated charges on particle surfaces. Thus, complete electric double layer could not form around the whole particle. In other words, counterion polarization can be distinguished from the two relaxations observed in our work. Many studies have found that the relaxation caused by the MW polarization usually appears around 10^2–10^5 Hz (Hao et al. 2001) when particles disperse in silicon oil. Therefore, the low-frequency relaxation around kilohertz can be considered to be caused by MW polarization. On the other hand, concerning the relaxation mechanism of higher frequency shown in Fig. 3, it may be interpreted as a new polarization caused intrinsically by the charging of the particle surface: when a particle was dispersed in a non-aqueous medium without added salts, the functional groups on the surface of particles will interact with the molecules of the medium and the charges on the functional groups are dissociated (Kitahara 1984). In our study, because the surface of TiO_2 particle had been treated with silica and gained active −OH group, when the particles were dispersed in silicone oil medium, the surface of particles will dissociate counterions such as OH^-. The dissociated ions are bound around the fixed charge and form ion pair with the fixed charges on TiO_2 surfaces. The fluctuation of the ion pair under ac field gave rise to the high-frequency relaxation around 0.1 MHz. Hereinafter, we will explain the mechanisms of the two relaxations with dielectric parameters in details.

Figure 5 shows the dependence of volume fraction of particles on relaxation time of low- (filled squares) and high- (open circles) frequency relaxations for rutile TiO_2 suspensions. It can be clearly seen that the relaxation time of low frequency is inversely proportional to particle concentrations. According to MW interface polarization theory, the

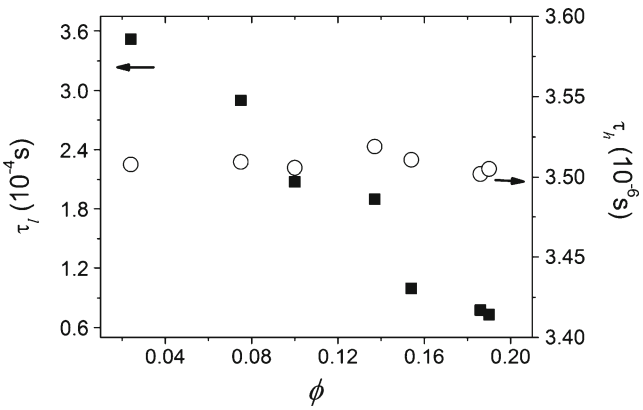

Fig. 5 Dependence of volume fraction of particles on relaxation time of low- (*filled squares*) and high- (*open circles*) frequency relaxations for rutile TiO_2 suspensions

relaxation time can be estimated by the following equation (Hanai et al. 1977):

$$\tau = \varepsilon_0 \frac{\left(\frac{2+\phi}{1-\phi}\right)\varepsilon_a + \varepsilon_p}{\left(\frac{2+\phi}{1-\phi}\right)\kappa_a + \kappa_p}. \quad (13)$$

Although we do not know the accurate values of κ_p now, according to literatures (Wang et al. 2007), the value of ε_p for rutile TiO_2 and the value of ε_a can be gained: they are ~100 and ~3, respectively. It means $\varepsilon_p \gg \left(\frac{2+\phi}{1-\phi}\right)\varepsilon_a$. Therefore, Eq. 13 can be simplified as

$$\tau = \varepsilon_0 \frac{\varepsilon_p}{\left(\frac{2+\phi}{1-\phi}\right)\kappa_a + \kappa_p}. \quad (14)$$

From Eq. 14, it is clear that the relaxation time is inversely proportional to the volume fraction, ϕ, of particle, being consistent with the result of Fig. 5. It is strongly suggested that the low-frequency relaxation is due to the interface polarization. With regard to the relaxation mechanism of high frequency, quite other than that at low frequency should be taken into account. From Fig. 5, it is also clear that relaxation time is almost independent with particle concentrations. It may also be considered to be caused by the permanent dipole moment of the silicone oil molecule. However, the relaxations of silicone oil do not appear in the frequency range of our study. As discussed above, the high-frequency relaxation around 0.1 MHz is considered to be a fluctuation of ion pair under an ac field. The relaxation time caused by fluctuation of ion pair is not very sensitive to volume fraction ϕ.

Figure 6 shows the dependence of volume fraction of particles on special dielectric increments $\Delta\varepsilon/\phi$ of low- (a) and high- (b) frequency relaxations for rutile (open squares), anatase (open circles), and mixed (open triangles) TiO_2 suspensions. The $\Delta\varepsilon/\phi$ indicates the relaxation strength of suspensions of particles per unit volume. From Fig. 6a, it can be seen that the special dielectric increments of low-frequency relaxation, $\Delta\varepsilon_l/\phi$, are roughly independent with volume fraction and the values of $\Delta\varepsilon_l/\phi$ for the three types of TiO_2 suspensions are different from one another.

According to MW interface polarization theory (Hanai et al. 1977), the dielectric increment for a suspension can be given by

$$\Delta\varepsilon = 9\phi \frac{\left(\varepsilon_p\kappa_a - \varepsilon_a\kappa_p\right)^2 (1-\phi)}{\left[(1-\phi)\varepsilon_p + (2+\phi)\varepsilon_a\right]\left[(1-\phi)\kappa_p + (2+\phi)\kappa_a\right]^2}. \quad (15)$$

Because the values of volume fraction of this study are small, Eq. 15 can be reexpressed as

$$\Delta\varepsilon/\phi = 9\frac{\left(\varepsilon_p\kappa_a - \varepsilon_a\kappa_p\right)^2}{\left(\varepsilon_p + 2\varepsilon_a\right)(\kappa_p + 2\kappa_a)^2}. \quad (16)$$

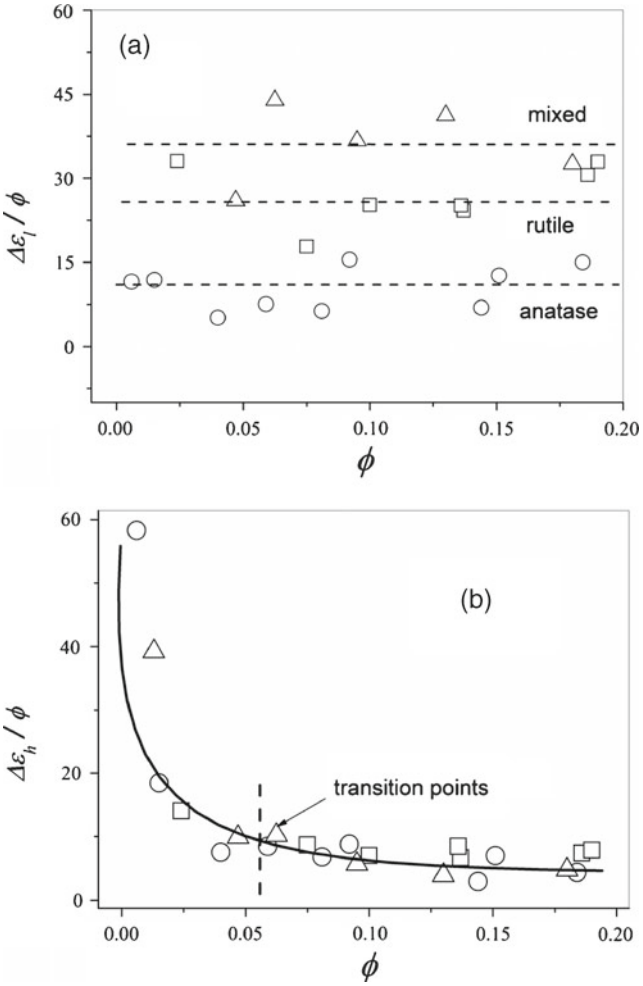

Fig. 6 Dependence of volume fraction of particles on special dielectric increments of low- (**a**) and high- (**b**) frequency relaxations for rutile (*open squares*), anatase (*open circles*), and mixed (*open triangles*) TiO_2 suspensions. The *lines* or *dash line* are drawn to guide the eyes

Equation 16 shows that the special dielectric increment, $\Delta\varepsilon/\phi$, is determined by the permittivity, ε_p and ε_a, and the conductivity, κ_p and κ_a, of suspended particles and continuous aqueous medium and the values of $\Delta\varepsilon/\phi$ should be approximately independent with volume fraction ϕ. This is in agreement with the result shown in Fig. 6a.

About the special dielectric increments of high-frequency relaxation, $\Delta\varepsilon_h/\phi$, its dependence on ϕ is completely different from that of low-frequency relaxation as shown in Fig. 6b: the dependence has almost nothing to do with TiO_2 polymorphs. This indicates that the relaxation mechanism of high frequency is different from that of low-frequency relaxation in a new way, supporting the conclusion on high-frequency relaxation mechanism discussed above. From another perspective, because the surface of TiO_2 used in this work all gained −OH due to surface treatment, all the TiO_2

particles have almost the same surface properties, resulting in the generation of the same or similar dissociated and fixed charges. Therefore, the conclusion that the mechanism of high frequency is independent with TiO_2 polymorphs is reasonable.

As for the change of $\Delta\varepsilon_h/\phi$ with increasing ϕ, we may have the following interpretations: As volume fraction of particles increased, the aggregation and interaction between nanoparticles may lead to the decrease of the number of effect dissociated charges per unit volume; thus, the values of $\Delta\varepsilon/\phi$ are decreased. However, the decreases slow down after ϕ is about 0.05, suggesting that a more complex structure such as networks has formed. The discussion detail of structure change of suspensions will be stated below.

Structure changes of TiO_2-based ER suspensions

During the preparation of TiO_2 suspensions, it can be observed that the state of suspensions transform from liquid-like to a solid-like as particle volume fraction increased. This critical volume fraction ϕ_c of phase transition is about 0.05, which coincides with the point observed in Fig. 6b. This phenomenon suggests that the structure of the suspensions has undergone some changes, such as aggregation and formation of chain-like or network structures by particles. And the structure changes can be detected by dielectric properties.

Figure 7 shows the dependence of volume fraction of particles on limiting permittivity at low-frequency ε_l for rutile (open squares), anatase (open circles), and mixed (open triangles) TiO_2 suspensions. From Fig. 7, it can be seen that ε_l increases with ϕ over the particle concentration range of

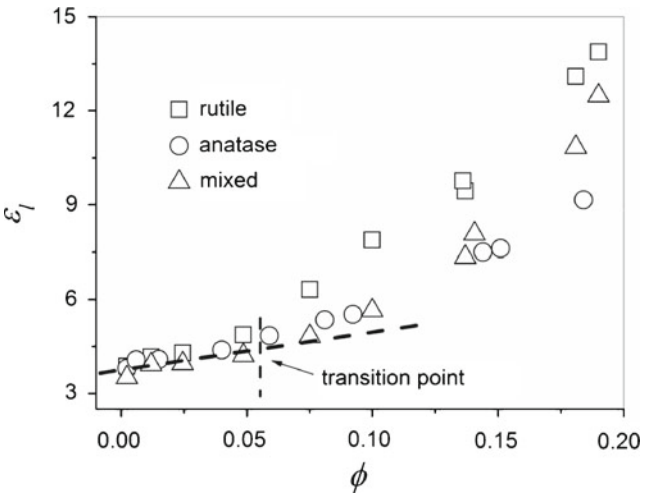

Fig. 7 Dependence of volume fraction of particles on limiting permittivity at low frequency for rutile (*open squares*), anatase (*open circles*), and mixed (*open triangles*) TiO_2 suspension. The *dash lines* are drawn to guide the eyes

this work and there is a transition point near $\phi_c \approx 0.05$ for all types of TiO_2 suspensions in this concentration range. This suggests that structures or interactions between particles must undergo profound changes around this volume fraction.

In order to explain the transition point of low-frequency permittivity in Fig. 7, a formula (Grosse and Shilov 2007) (Eq. 17) describing the relation between the low-frequency permittivity and volume fraction of particles of a colloid system was employed:

$$\varepsilon_l = \varepsilon_a(1 + 3\phi D) \tag{17}$$

where D is the dipolar coefficient and the definitions of ε_l, ε_a, and ϕ are all the same with those defined above. According to Eq. 17, the low-frequency permittivity ε_l should linearly increase with ϕ, being consistent with the dependence of ϕ on ε_l before or after the transition point ϕ_c (critical volume fraction) as can be seen in Fig. 7. It should be noted here that there are different slopes before and after ϕ_c. This indicates that dipolar coefficient D is different before and after ϕ_c. Considering the fact that the dipolar coefficient D is related to the construction or structure of the colloid system, the changes of D may be ascribed to the aggregation and formation of chain-like or network structures by particles. It should be stated that the critical volume fraction ϕ_c of typical spherical particle suspensions is about 0.494 (Cheng et al. 1999). Compared to the typical suspension, ϕ_c obtained in this work is very small. This may be attributed to the size and the anisotropic of particles in the suspension. The anisotropic of the particles comes from the fractal-like aggregated clusters (Balberg et al. 1984).On the other hand, the small ϕ_c also may be due to high surface energy of nanoparticles. This can be interpreted by the concept of "jamming" (Liu and Nagel 1998). Jamming is a phenomenon to describe phase transition from a liquid-like state to a solid-like state as volume fraction increases. According to the jamming phase diagram (Trappe et al. 2001), "jamming transition" of suspensions will occur at low volume fraction when energy is high. However, jamming may cause a negative effect on ER activity, because in practical application, ER fluid should be kept in a liquid-like state when electric field is absent.

Figure 8 shows the dependence of volume fraction of particles on limiting conductivity κ_1 at low frequency for rutile (open squares), anatase (open circles), and mixed (open triangles) TiO_2 suspensions. It is obvious that Fig. 8 gave a similar variation trend of $\kappa_1 \sim \phi$ curve with that of $\varepsilon_l \sim \phi$ curve, i.e., κ_1 increases with ϕ over the particle concentration range and the rate of the increase is different before and after $\phi \approx 0.05$. A concept, so-called "percolation" (Safran et al. 1995; Stauffer 1985), is always referred to interpret the influence of volume fraction of particles on physical properties of colloid. According to the percolation theory, a

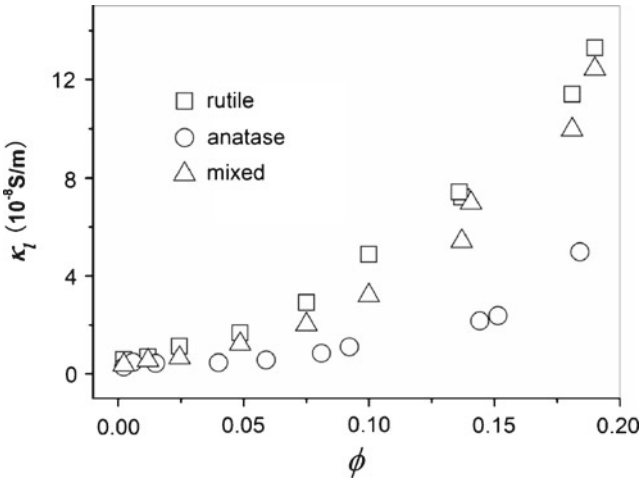

Fig. 8 Dependence of volume fraction of particles on limiting conductivity at low frequency for rutile (*open squares*), anatase (*open circles*), and mixed (*open triangles*) TiO_2 suspensions

universal relationship between the conductivity and volume fraction of particles can be expressed as (Stauffer 1985)

$$\kappa \propto (\phi - \phi_c)^t \quad \text{at} \quad \phi > \phi_c \tag{18}$$

where t is the critical exponent, depending on the topological dimensionality, d, of the disordered system. According to the percolation theory, the value for t is 1.3 and 2.0 in two dimensions ($d = 2$) and three dimensions ($d = 3$), respectively (Hunt and Ewing 2009). From Eq. 18, we can obtain the values of t and the fitting results are shown in Fig. 9.

Figure 9 gave us the values of the critical exponent t: 0.850 for rutile, 1.034 for mixed, and 1.149 for anatase TiO_2 suspensions. We note that the values of t for the three polymorphs of TiO_2 suspensions are all inconsistent with and smaller than the theoretical values (either 1.3 for

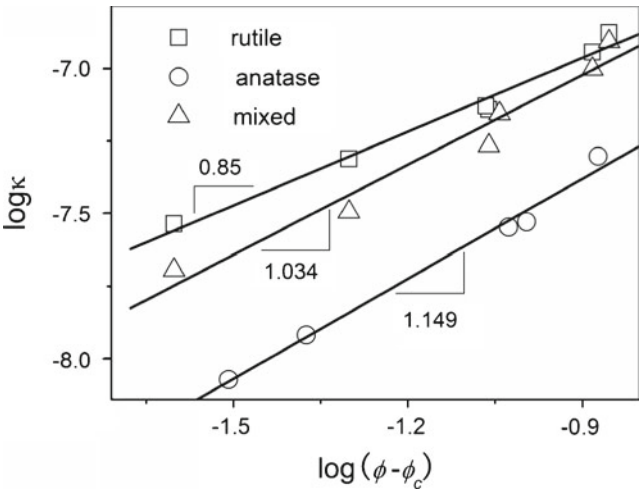

Fig. 9 Log–log plot of the conductivity vs. (ϕ–ϕ_c) for rutile (*open squares*), anatase (*open circles*), and mixed (*open triangles*) TiO_2 suspensions. The *solid line* is the best fit to Eq. 18

$d = 2$ or 2.0 for $d = 3$). This indicates that the percolation theory is not valid for TiO_2 suspensions. This is probably due to the non-conductivity properties of TiO_2 particles. Here, we explained as follows: The phenomenon of conductance percolation always occurs in binary mixtures containing conductor and insulator. In such systems, conductive particles can form chain-like or network structures after a critical volume fraction. Chains or network structures supply ion transfer channels, resulting in a sharp increase of conductivity and the universal relationship, i.e., Eq. 18, between the conductivity and particle volume fraction. In the present work, TiO_2 particles and silicon oil are all non-conductive. Therefore, although particles form aggregate or chain-like structures, the inherent non-conductivity properties of particles cannot generate significant conductance percolation phenomenon. However, the values of t for anatase TiO_2 suspension are close to the 1.3, suggesting that the anatase TiO_2 particles may form two-dimensional chain-like or network aggregation.

Phase parameters and effective dielectric mismatch parameters of TiO_2 suspensions

Phase parameters of TiO_2 suspensions

The phase parameters for all the systems were obtained by means of Hanai's method and Eq. 8 described in "Dielectric model and determination of phase parameters". Some of the obtained phase parameters are listed in Table 2. In Table 2, β_d and β_c are dielectric and conductivity mismatch parameters, respectively. Detailed calculation process and discussion of β_d and β_c will be interpreted in "Effective dielectric mismatch parameters and ER effect of TiO_2 suspensions".

Figure 10 shows the dependences of volume fraction of particles on the permittivity (a) and conductivity (b) for rutile, mixed, and anatase TiO_2 suspensions. From Fig. 10, it is clear that both the values of permittivity ε_p and conductivity κ_p of particle are in the order of rutile > mixed > anatase at any ϕ. Generally speaking, according to literature (Wang et al. 2007, 2010; Yang et al. 2006; Lee et al. 1999), the permittivity of TiO_2 particle in suspension is always influenced by many factors including its topography, and its

Table 2 Dielectric parameters and mismatch parameters for 25 wt% TiO_2 suspensions

TiO_2 polymorph	ε_p	κ_p(S/m)	ε_a	κ_a(S/m)	β_d^2	β_c^2
Rutile	105	2.50E−7	3.50	5.20E−8	0.823	0.313
Anatase	47.1	3.06E−8	3.50	1.01E−8	0.649	0.163
Mixed	65.7	1.02E−7	3.50	5.01E−8	0.732	0.0663

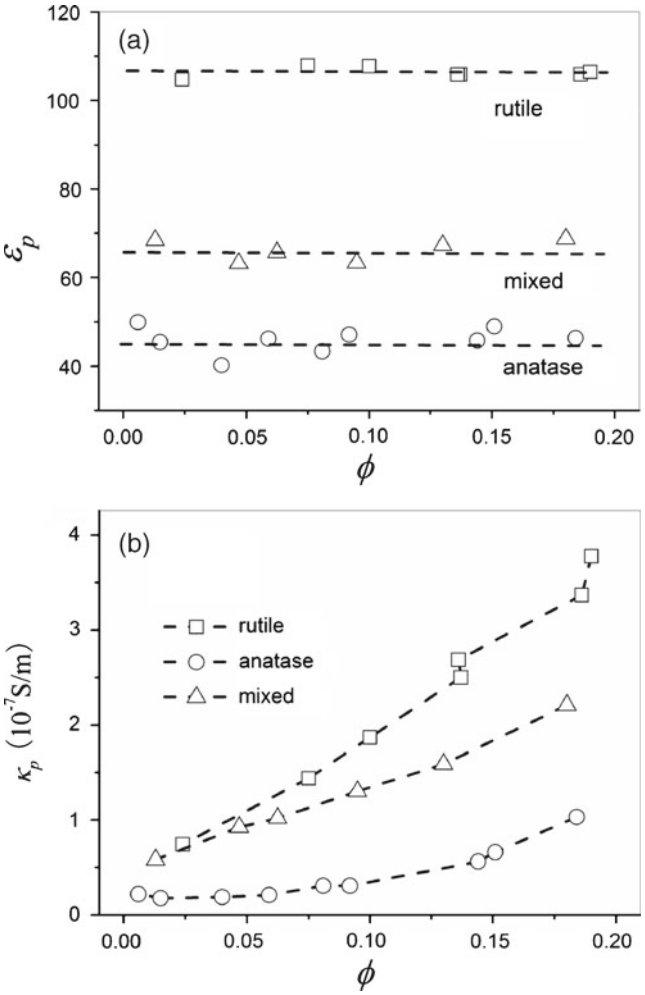

Fig. 10 Dependences of volume fraction of particles on the permittivity (**a**) and conductivity (**b**) for rutile (*open squares*), mixed (*open triangles*), and anatase (*open circles*) TiO_2 suspensions

values reported in different literatures are different from one another. As for the ε_p obtained in this work, it is almost independent with volume fraction ϕ of particles, indicating that ε_p is determined mainly by the inherent property of particles. It should be noticed here that the electric field strength used in dielectric measurement is very small. When particles, however, are under a strong field, for instance, when the suspension is applied as an ER fluid, the situation is totally different. The strong local field and the interactions between particles may change the polarization and hence the permittivity of particles when ϕ is high. On the other hand, the obtained conductivity κ_p increases with ϕ. This may be due to the increase in the numbers of ion pairs between dissociated counterions and fixed charges on particle surfaces with ϕ. More ion pairs fluctuated on the surface of particles under electric field, which increases the effective conductivity of particles.

In the following section, the calculation of the effective dielectric mismatch parameters based on phase parameters and the ER effect of TiO_2 suspensions will be discussed.

Effective dielectric mismatch parameters and ER effect of TiO_2 suspensions

As mentioned previously, the ER effect of a fluid is due to the formation of chain-like structure by particles (Winslow 1949). The polarization model is the most acceptable mechanism to explain the formation of chain-like structure and is applied by many studies. According to this model, ER effect is contorted by dielectric mismatch between the particles and continuous medium of fluid. Under a dc electric field, particles in suspension will be polarized to generate a force between neighboring particles; the force, F, can be expressed as (Parthasarathy and Klingenberg 1996; Espin et al. 2007)

$$F = -12\pi\varepsilon_0\varepsilon_a a^2\beta_d^2 E^2\left(\frac{a}{r}\right)^4\left[(3\cos^2\theta - 1)\,\widehat{e}_r + (\sin\,2\theta)\widehat{e}_\theta\right] \tag{19}$$

where a is the radius of particle and r is the distance between two particles. θ is the angle between the line connecting the spheres and the field direction, $\widehat{e}_r$ and $\widehat{e}_\theta$ are the unit vectors in r and θ direction, respectively. β is the dielectric mismatch parameter:

$$\beta_d = \frac{\varepsilon_p - \varepsilon_a}{\varepsilon_p + \varepsilon_a}. \tag{20}$$

According to Eq. 19, the force, F, is in proportion to β_d^2. Therefore, the higher the β_d^2, the stronger the interaction force is. The stronger interaction force will produce better ER effect. The values β_d^2 of TiO_2 suspensions swing between 0.6 and 0.9 (see Table 2). This suggests a good ER activity for TiO_2 suspensions. However, rheological studies (Yin and Zhao 2006; Wang et al. 2007) have found that the ER activity of pure TiO_2 is very weak. This shows that the polarization model is not valid for pure TiO_2 suspensions. To explain the particularity of TiO_2-based ER suspensions, effective dielectric mismatch (Parthasarathy and Klingenberg 1996; Espin et al. 2007), which considers the effect of conductivity of constituents of suspensions and frequency of electric field on dielectric mismatch, was employed:

$$\beta_{eff}^2 = \frac{\beta_c^2 + \beta_d^2\,(\omega\tau_{MW})^2}{1 + (\omega\tau_{MW})^2} \tag{21}$$

where $\beta_c\left(=\frac{\kappa_p-\kappa_a}{\kappa_p+2\kappa_a}\right)$ is the conductivity mismatch, $\beta_d = \frac{\varepsilon_p-\varepsilon_a}{\varepsilon_p+\varepsilon_a}$, and $\tau_{MW} = \varepsilon_0\frac{\varepsilon_p+2\varepsilon_a}{\kappa_p+2\kappa_a}$ is the MW relaxation time.

Combining the phase parameters (ε_p, κ_p, ε_a, κ_a) in Table 2 and Fig. 10, we can obtain a set data of β_c, β_d, and τ_{MW} at each particle volume fraction. Thus, in Eq. 21, ω is

the only independent variable for β_{eff}. Therefore, the dependence of effective dielectric mismatch, β_{eff}, on frequency of electric field can be calculated.

Figure 11 shows the calculation curves of β_{eff}^2 as function of frequency of electric field for the suspensions of TiO_2 particle with different polymorphs. It can be seen that the values of β_{eff}^2 for all TiO_2 suspensions are small in low-frequency range. As frequency increased, β_{eff}^2 sharply increased and reached a new steady value at high-frequency range. The small values of β_{eff}^2 at low frequency indicate that when a very low frequency of external alternating field (under a few hertz), equivalent to a dc field, was applied to the suspension, the interaction force between the particles in suspension is not strong enough to form chain-like structures and the suspension cannot gain good ER activity. On the other hand, when the applied alternating field frequency is sufficiently high, the polarization of particles cannot follow the change of the field; as a result, the particles only become randomly distributed by small clusters (Espin et al. 2007; Wen et al. 2000). For this reason, although β_{eff}^2 at high frequency is large enough to lead to strong interaction force between the particles, the randomly distributed clusters still decrease the ER activity because the particles cannot form chain-like structure between electrodes. Therefore, ER activity of pure TiO_2 suspensions is poor as reported by experimental studies about ER activity of pure TiO_2 (Yin and Zhao 2006; Wang et al. 2007). It should be noticed that at low frequency, β_{eff}^2 approaches β_c^2, while at high frequency, β_{eff}^2 goes to β_d^2 (e.g., for rutile suspension, $\beta_c^2 = 0.313$, $\beta_d^2 = 0.813$, at low frequency $\beta_{eff}^2 = 0.312$, at high frequency $\beta_{eff}^2 = 0.822$). It means that ER effect is controlled by conductivity mismatch β_c^2 at low frequency while the dielectric mismatch β_d^2 at high frequency. From Table 2, it can be seen that β_c^2 is much smaller than β_d^2 for the all suspensions of different TiO_2 polymorphs. In other words, the low value of β_c^2 may be the critical factor to result in poor ER activity of TiO_2 suspensions. Therefore, to enhance ER activity of TiO_2, improving the conductivity properties of TiO_2 should be preferred. The conductivity of pure TiO_2 crystals can be altered by many ways, such as mixing metals or ions (Yin and Zhao 2006), adding conducting polymers (Cheng et al. 2009), and enhancing mesoporous structures or surface properties (Yin and Zhao 2002, 2004, 2006; Wang et al. 2007) of particles.

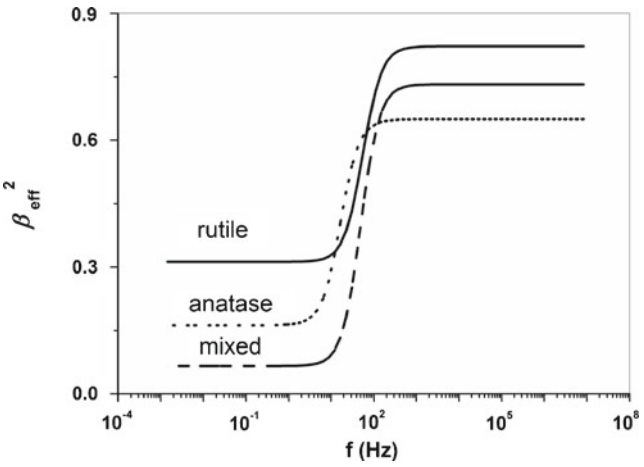

Fig. 11 Calculation curves of square of effective dielectric mismatch, β_{eff}^2, as function of frequency of electric field for TiO_2 suspensions with different TiO_2 polymorphs. The concentration of suspension is 25 wt%

Moreover, it is also clear from Fig. 11 that the values of β_{eff}^2 for rutile TiO_2 suspensions are larger than that of anatase TiO_2 suspensions, indicating that rutile have better ER activity than anatase. Since most of TiO_2 used in literatures is anatase (Liu et al. 2010; Yin and Zhao 2006; Cheng et al. 2009; Wang et al. 2007), further rheological experimental confirmation is needed.

Conclusion

Dielectric behaviors of TiO_2-based ER suspensions with different concentration of particles and different TiO_2 polymorphs were investigated in the frequency range from 40 Hz to 110 MHz. Two relaxations in kilohertz and megahertz frequency range for all the studying systems were observed.

Through comparing the dependence of dielectric parameters of the two relaxations on volume fraction ϕ of particles, the low-frequency relaxation around kilohertz and the high-frequency relaxation about 0.1 MHz were determined to be caused by interface polarization between the TiO_2 particle and silicone oil and the polarization of the ion pair, which form between dissociated counterions and fixed charges on TiO_2 surfaces, respectively. The dependence of low-frequency limiting permittivity ε_1 on ϕ shows that the dipolar coefficient D is related to the construction or structure of the colloid system and changes after critical volume fraction $\phi_c \approx 0.05$, indicating that chain-like or network structures are formed by particles after ϕ_c. According to the percolation theory and the relationship between low-frequency limiting conductivity κ_1 and ϕ (Eq. 18), the obtained values of critical exponent t indicate that the percolation model is not available to TiO_2 suspensions because of non-conductivity properties of TiO_2 particles. However, the values of t are close to 1.3, suggesting that the particles may form two-dimensional chain-like or network aggregation at least.

The phase parameters characterizing the electrical properties of dispersed particles in suspension were calculated by using Hanai's method. Furthermore, according to the modified polarization models, the effective dielectric mismatch parameter, β_{eff}, was calculated based on the obtained

phase parameters. We found that the main reason for the weak ER activity of pure TiO_2-based ER suspensions is due to the poor conductivity properties of TiO_2 crystals. Therefore, to enhance ER activity of TiO_2, improving the conductivity properties of TiO_2 should be preferred. Moreover, by comparing with the values of β_{eff}^2 between rutile and anatase, we found that rutile should have better ER activity than anatase. However, further rheological experimental confirmation is needed.

We have presented a set of experimental data and gain valuable parameters on the structure changes and electrorheological properties of TiO_2-based ER suspensions. The results supplied an actual example for predicting electrorheological properties of suspensions just by dielectric analysis.

Acknowledgment Financial support of this work by the National Natural Science Foundation of China (nos. 21173025 and 20976015) is gratefully acknowledged.

References

Balberg I, Binenbaum M, Wagner N (1984) Percolation thresholds in the three-dimensional sticks system. Phys Rev Lett 52:1465

Cheng QL, Pavlinek V, He Y, Li CZ, Saha P (2008) Structural and electrorheological properties of mesoporous silica modified with triethanolamine. Colloids Surf A Physicochem Eng Asp 318:169–174

Cheng QL, Pavlinek V, He Y, Li CZ, Saha P (2009) Electrorheological characteristics of polyaniline/titanate composite nanotube suspensions. Colloid Polym Sci 287:435–441

Cheng Z, Russel WB, Chalkin PM (1999) Controlled growth of hard-sphere colloidal crystals. Nature 401:893–895

Cole KS, Cole RH (1941) Dispersion and absorption in dielectrics. I. Alternating current characteristics. J Chem Phys 9:341–351

Dukhin SS, Shilov VN (1974) Dielectric phenomena and the double layer in disperse systems and polyelectrolytes. Wiley, New York

Espin MJ, Delgado AV, González-Caballero F, Rejon L (2007) Rheological properties of a model colloidal suspension under large electric fields of different waveforms. J Non-Newton Fluid Mech 146:125–135

Grosse C, Shilov VN (2007) Dependence of the dielectric properties of suspensions on the volume fraction of suspended particles. J Colloid Interface Sci 309:283–288

Hanai T, Imakita A, Koizumi N (1977) Systematic analysis to determine of dielectric phase parameters from dielectric relaxations caused by diphasic structure of disperse systems. Bull Inst Chem Res Kyoto Univ 55:4

Hao T (2001) Electrorheological fluids. Adv Mater 13(2001):1847–1857

Hao T (2002) Electrorheological suspensions. Adv Colloid Interface Sci 9:71–35

Hao T, Kawai A, Ikazaki F (2001) Direct differentiation of the types of polarization responsible for the electrorheological effect by a dielectric method. J Colloid Interface Sci 239:106–112

Havriliak S, Negami S (1967) A complex plane representation of dielectric and mechanical relaxation processes in some polymers. Polymer 8:161–210

Hunt A, Ewing R (2009) Percolation theory for flow in porous media. Springer, Berlin, p 43

Ikazaki F, Kawai A, Kawakami T (1998) Mechanisms of electrorheology: the effect of the dielectric property. J Phys D Appl Phys 31:336

Klass DL, Martinek TW (1967) Electroviscous fluids. I. Rheological properties. J Appl Phys 38:67

Kitahara A (1984) Nonaqueous systems. In: Kitahara A, Watanabe A (eds) Electrical phenomena at interfaces. Marcel Dekker, New York, p 119

Labat F, Baranek P, Domain C, Minot C, Adamo C (2007) Density functional theory analysis of the structural and electronic properties of TiO_2 rutile and anatase polytypes: performances of different exchange-correlation functionals. J Chem Phys 154703:126

Lee BH, Jeon Y, Zawadzki K, Qi WJ, Lee J (1999) Effects of interfacial layer growth on the electrical characteristic of thin titanium oxide films on silicon. Appl Phys Lett 74:3143

Liu AJ, Nagel SR (1998) Jamming is not just cool anymore. Nature 396:21–22

Liu FH, Xu GJ, Wu JH, Cheng YC, Guo JJ, Cui P (2010) Synthesis and electrorheological properties of oxalate group-modified amorphous titanium oxide nanoparticles. Colloid Polym Sci 288:739–1744

Parthasarathy M, Klingenberg DJ (1996) Electrorheology: mechanisms and models. Mater Sci Eng R 17:57–103

Safran SA, Webman I, Grest GS (1995) Percolation in interacting colloids. Phys Rev A 32:506–511

Schönhals A, Goeing H, Costa FR, Wagenknecht U, Heinrich G (2009) Dielectric properties of nanocomposites based on polyethylene and layered double hydroxide. Macromolecules 42:4165–4174

Schwan HP (1963) Determination of biological impedance. In: Nastuk WL (ed) Physical techniques in biological research, vol 6. Academic, New York, p 373

Stangroom JE (1983) Electrorheological fluids. Phys Technol 14:290

Stauffer D (1985) Introduction to percolation theory. Taylor & Francis, London

Trappe V, Prasad V, Cipelletti L, Segre PN, Weitz DA (2001) Jamming phase diagram for attractive particles. Nature 411:772–775

Van Beek LKH (1967) Dielectric behaviour of heterogeneous systems. In: Birks JB (ed) Progress in dielectrics, vol 7. Heywood Books, London, pp 69–114

Wang BX, Zhao Y, Zhao XP (2007) The wettability, size effect and electrorheological activity of modified titanium oxide nanoparticles. Colloids Surf A Physicochem Eng Asp 295:27–33

Wang HT, Xu S, Gordon RG (2010) Low temperature epitaxial growth of high permittivity rutile TiO_2 on SnO_2. Electrochem Solid-State Lett 13(9):G75–G78

Wen WJ, Ma HR, Tam WY, Sheng P (2000) Frequency-induced structure variation in electrorheological fluids. Appl Phys Lett 77:3821–3823

Winslow WM (1949) Induced fibration of suspensions. J Appl Phys 20:1137

Yang WL, Marino J, Monson A, Wolden CA (2006) An investigation of annealing on the dielectric performance of TiO_2 thin films. Semicond Sci Technol 21:1573–1579

Yin JB, Zhao XP (2002) Preparation and electrorheological activity of mesoporous rare-earth-doped TiO_2. Chem Mater 14:4633–4640

Yin JB, Zhao XP (2004) Giant electrorheological activity of high surface area mesoporous cerium-doped TiO_2 templated by block copolymer. Chem Phys Lett 398:393–399

Yin JB, Zhao XP (2006) Enhanced electrorheological activity of mesoporous Cr-doped TiO_2 from activated pore wall and high surface area. J Phys Chem B 110:12916–12925

Zhao KS, Asami K, Lei JP (2002) Dielectric analysis of chitosan microsphere suspensions: study on its ion adsorption. Colloid Polym Sci 280:1038–1044